

# Continuous and high throughput production of alginate fibers using co-flow in a millifluidic T-junction

G. Pendyala, S. S. Bithi, S. A. Vanapalli, G. E. Fernandes

Department of Chemical Engineering, Texas Tech University, Lubbock, Texas 79409-3121

Correspondence to: G. E. Fernandes (E-mail: gregory.fernandes@ttu.edu)

**ABSTRACT:** We present a new technique for continuous production of alginate fibers using off-the-shelf millifluidic components and syringe pumps. The components are quickly assembled to form a T-junction to deliver co-flowing streams of sodium alginate and calcium chloride allowing formation of hydrogel fibers in the exit channel. We vary the flow rates of the two streams, calcium chloride concentrations and length of exit channel and identify conditions where fibers of uniform and nonuniform thickness are produced. We find that uniform fibers can be produced at a maximum total flow rate of  $10 \text{ mL min}^{-1}$ . As expected, for uniform fibers, we observe that the fiber diameter increases with increase in alginate solution flow rate, and we propose a simple model that predicts the fiber diameter as a function of flow rate ratio. We investigate the source of fiber nonuniformity and explain it using an empirical model that involves crosslinking time and gel strength. Our approach features easy device assembly and operation and enables continuous fiber production without clogging risks. Fiber production rates in the order of  $10 \text{ m min}^{-1}$  are achievable using our approach. © 2018 Wiley Periodicals, Inc. *J. Appl. Polym. Sci.* **2018**, 00, 47120.

**KEYWORDS:** alginate; fiber; hydrogel; T-junction

Received 20 May 2018; accepted 19 August 2018

DOI: 10.1002/app.47120

## INTRODUCTION

Alginate fibers are attractive candidates for use in tissue engineering<sup>1–4</sup> and wound management<sup>5–7</sup> due to their nontoxicity and biocompatibility. A common approach in tissue engineering is to weave,<sup>1</sup> knit,<sup>2</sup> or braid alginate fibers into scaffolds followed by cell seeding. Alternatively, cell encapsulation inside alginate fibers is carried out first, followed by scaffold fabrication.<sup>3</sup> Alginate fibers are also used to make wound dressings. Dressings made from calcium alginate fibers swell on contact with wound exudate and provide a moist environment that facilitates wound healing.<sup>5,6</sup>

Electrospinning,<sup>8–12</sup> wet spinning,<sup>7,9,13–15</sup> microfluidic spinning,<sup>9,16–24</sup> interfacial complexation,<sup>9,25–28</sup> and millifluidic jetting<sup>29</sup> are some of the existing methods used to make alginate fibers. Device clogging is a concern when using microfluidic spinning techniques<sup>9,16–24</sup> since the gelation time is rapid and can only be resolved by incorporating declogging measures which make these devices more difficult to fabricate and operate. Microfluidic techniques also suffer from low fiber production rates. Other methods like electrospinning<sup>8–12</sup> cannot be used to encapsulate cells because they use harsh solvents and high electric fields ( $\sim 1\text{--}2 \text{ kV cm}^{-1}$ ).

Here, we present a simple “plug-and-play” millifluidic device which consists of a commercially available T-junction and three

connected Tygon tubes. Using syringe pumps, we flow sodium alginate and calcium chloride solutions through tubes connected to two ends of the T-junction. The T-junction delivers co-flowing alginate and calcium chloride streams at its exit, forming alginate hydrogel fibers. Without any fabrication step, this “plug-and-play” method can produce alginate fibers with a wide range of thickness ( $300\text{--}1000 \text{ }\mu\text{m}$ ) at relatively fast fiber production rates ( $\sim 1 \text{ m min}^{-1}$ ).

Our technique has several features that address some of the drawbacks of previously reported methods, namely: (1) the millimeter scale does not present clogging issues even though the gelation time is rapid, (2) simple assembly without any fabrication step due to the use of commercially available parts and equipment for fiber production, (3) no toxic chemicals used during fiber production, and (4) fast fiber production rates due to operation at the millimeter scale.<sup>9,29,30</sup> In addition, unlike prior microfluidic work on fiber production,<sup>22,24,29</sup> our work also presents simple models that allow prediction of fiber diameter and regime of uniform fiber production.

In this report, we use our simple “plug-and-play” device to: (1) explore the operating conditions that produce uniform alginate fibers, (2) show that flow rate ratio of alginate to calcium

chloride solutions (R) controls fiber diameter, (3) demonstrate that fiber production rate is also dependent on R, and (4) explore the effect of crosslinking time on fiber quality. Our simple “plug and play” milli-device technique has the potential to produce uniform high throughput alginate fibers for diverse applications in tissue engineering and wound management.

## EXPERIMENTAL

### Materials

All chemicals are used as received. Calcium chloride (anhydrous powder) is purchased from Sigma-Aldrich (St. Louis, MA) and VWR (Radnor, PA). Alginate acid (sodium salt) is purchased from Sigma-Aldrich. T-Junctions (200 Series Barbs, 1/16" ID, Clear Polycarbonate) are purchased from Nordson Medical (Westlake, OH). Flexible plastic tubing (Tygon microbore tubes, 0.050" ID and 0.090" OD) is purchased from Cole Palmer (Vernon Hills, IL). Plastic syringes (BD 10, 30, and 60 mL, Luer-Lok tip) are purchased from Becton Dickinson (East Rutherford, NJ).

### Millifluidic Setup for Calcium Alginate Fiber Production

Figure 1 describes the experimental setup used to produce alginate fibers. Three plastic tubes are connected to the three ends of the T-junction [Figure 1(a,b)]. Tubes connected to the two horizontal ends of the T-junction function as inlet channels and the tubing connected to the vertical end of the T-junction acts as the exit channel for alginate fibers. A vertical exit channel is chosen as it minimizes transverse mixing caused by density differences between the co-flowing streams. Syringe pumps (Harvard apparatus PHD 2000) deliver constant flow rates of sodium alginate ( $\dot{Q}_{\text{Alg}}$ ) and calcium chloride ( $\dot{Q}_{\text{CaCl}_2}$ ) solutions to the T-junction. The T-junction delivers co-flowing streams of sodium alginate and calcium chloride through the exit channel [Figure 1(b,c)] where alginate is crosslinked by calcium ions, forming an alginate hydrogel fiber. Alginate crosslinking time is controlled by using well-defined exit channel lengths ( $L$ ). Hydrogel fibers formed in the exit channel are collected and stored overnight in a calcium chloride solution.

The experiments are conducted at Reynolds numbers,  $Re < 300$  and Peclet number,  $Pe > 9000$ ; Here Reynolds number and Peclet number are defined as  $Re = \frac{\rho u d}{\mu}$  and  $Pe = \frac{uL}{D}$ , respectively, where,

$d$  is the width of the alginate or calcium chloride streams in the exit channel,  $u \left( = \frac{\dot{Q}}{A} \right)$  is the average velocity of the fluid flow through the exit channel,  $\rho$  is the density of alginate or calcium chloride solutions ( $\rho_{\text{Alg}} = 1.05 \text{ g mL}^{-1}$ ,  $\rho_{1\% \text{CaCl}_2} = 1.065 \text{ g mL}^{-1}$ , and  $\rho_{6\% \text{CaCl}_2} = 1.10 \text{ g mL}^{-1}$ ),  $\mu$  is the viscosity of alginate or calcium chloride solutions ( $\mu_{\text{Alg}} = 250 \text{ mPa s}^{-1}$ ,<sup>25</sup>  $\mu_{1\% \text{CaCl}_2} = 1.18 \text{ mPa s}^{-1}$  and  $\mu_{6\% \text{CaCl}_2} = 1.42 \text{ mPa s}^{-1}$ ) and  $D$  is the diffusion coefficient of calcium chloride ( $D_{1\% \text{CaCl}_2} = 1.129 \times 10^{-5} \text{ cm}^2 \text{ s}^{-1}$  and  $D_{6\% \text{CaCl}_2} = 1.532 \times 10^{-5} \text{ cm}^2 \text{ s}^{-1}$ ).<sup>32</sup>

### Characterizing Fiber Quality, Dimensions, and Production Rate

Alginate fibers are equilibrated by overnight storage in a calcium chloride solution, after which the solution and fibers are placed in a Petri dish. To obtain a fair and comprehensive representation of overall fiber quality and dimensions, images of five different sections of the fiber are captured using a microscope (CKX41 and IX81 from Olympus, Eclipse Ti-U from Nikon). For each image captured, 8–10 diameter measurements are obtained. All fiber diameters reported in this article are averages from the pooled data (i.e., include diameter measurements on all images). The fiber diameters were measured using ImageJ software.

The length of alginate fiber collected during a 4 min time interval is used to estimate the fiber production rate. Production rates reported in this article are an average of three such measurements.

## RESULTS AND DISCUSSION

### Regimes of Alginate Fiber Production

To identify the optimal conditions that produce fibers with uniform diameters, we varied the flow rates of alginate ( $\dot{Q}_{\text{Alg}}$ ) and calcium chloride ( $\dot{Q}_{\text{CaCl}_2}$ ) solutions. We conducted these experiments at two different concentrations of calcium chloride 1 and 6 wt %. Figure 2 summarizes the effect of total flow rate ( $\dot{Q}_{\text{total}} = \dot{Q}_{\text{Alg}} + \dot{Q}_{\text{CaCl}_2}$ ) and flow rate ratio ( $R = \frac{\dot{Q}_{\text{Alg}}}{\dot{Q}_{\text{CaCl}_2}}$ ) on alginate fiber production. In general, we find three regimes: (1) uniform fibers: the cross section of the fiber is uniform along its length [Figure 2(a)]; (2) nonuniform fibers: kinks appear in

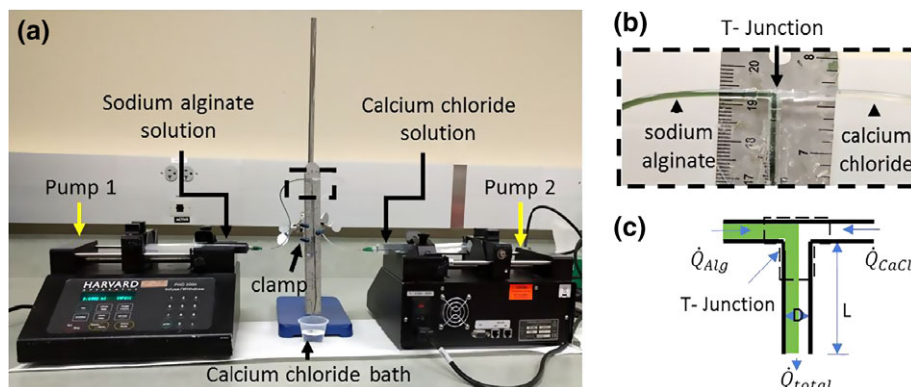


**Figure 1.** (a) Experimental setup for alginate hydrogel fiber production used in our study. (b) Enlarged image of the fiber production device used in our experiments [dotted area in (a)]. (c) Schematic description of the experimental setup to produce alginate fibers. [Color figure can be viewed at wileyonlinelibrary.com]

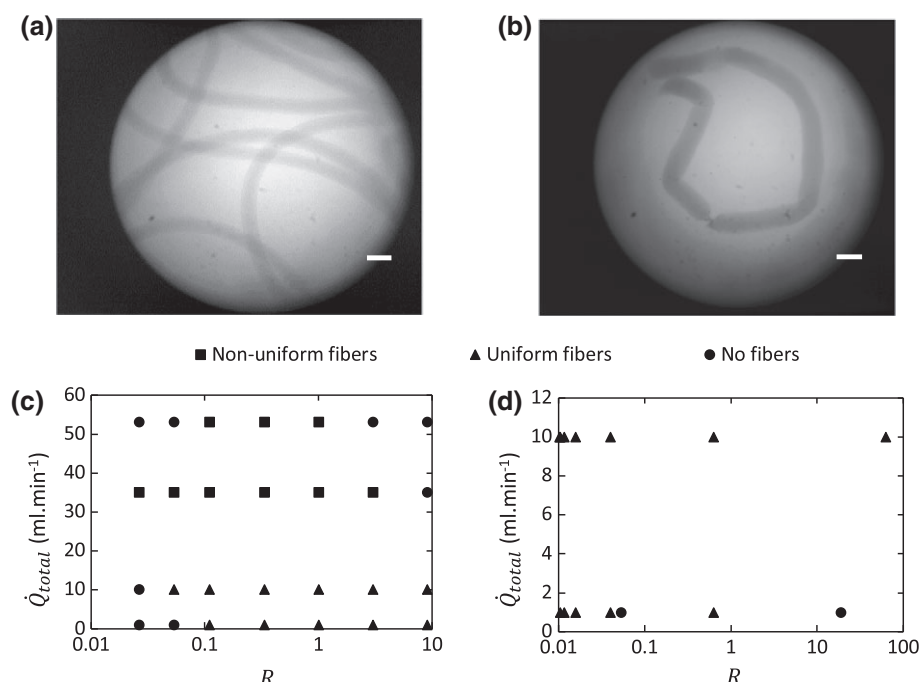


**Figure 2.** Representative images of (a) uniform and (b) nonuniform alginate hydrogel fibers produced by the millifluidic T-junction. (c) Operating conditions that produce uniform (▲) or nonuniform (■) fibers and conditions for which no fibers (●) are produced at 1 wt % CaCl<sub>2</sub>. (d) Operating conditions that produce uniform (▲) fibers and conditions for which no fibers (●) are produced at 6 wt % CaCl<sub>2</sub>.

the fiber [Figure 2(b)]; and (3) no fibers: the conditions did not generate any fibers.

As shown in Figure 2(c), at CaCl<sub>2</sub> concentration of 1 wt %, we observe that most of the conditions produce either uniform or non-uniform fibers with very few conditions not producing any fibers. The uniform fibers are produced at lower total flow rates and within  $0.1 < R < 10$ . At the higher CaCl<sub>2</sub> concentration of 6 wt %, we do not observe the production of non-uniform fibers and most of the conditions yield uniform fibers [Figure 2(d)]. Among the tested conditions, the maximum total flow rate at which uniform fibers can be produced in both cases is  $\dot{Q}_{total} = 10$  mL min<sup>-1</sup>. We note that the reason no fibers are produced at  $R < 1$  and  $\dot{Q}_{total} = 1$  mL min<sup>-1</sup> is because the calcium chloride stream enters the alginate inlet and plugs it. Likewise, for  $R \gg 1$  and  $\dot{Q}_{total} = 53$  mL min<sup>-1</sup>, the sodium alginate stream plugs the calcium chloride inlet, preventing fiber production. Use of a Y-junction in place of a T-junction may resolve some of these plugging issues but is beyond the scope of this work. In this work, we focused on exploring the range of operating parameters that allowed us to produce fibers using the simplest junction architecture (T-junction).

#### Dependence of Alginate Fiber Diameter and Production Rate on Flow Rate Ratio

It is expected that the fiber diameter will depend on the flow rate ratio as it determines both the residence time and the crosslinking time. To establish the dependence of the fiber diameter and production rate on the flow rate ratio, we selected the conditions where uniform fibers were produced and plot in Figure 3 the fiber diameter  $d_{fiber}$  normalized with the tube diameter  $D$ , as a

function of  $R$ . The results show that fiber diameter increases with increase in flow rate ratio and is independent of the total flow rates and CaCl<sub>2</sub> concentration. The actual fiber diameters obtained under these conditions ranged from 300 to 1000 nm.

To model the dependence of fiber diameter on flow rate ratio, we assume that the cross section of the alginate fiber is proportional to the flow fraction of the alginate. Therefore

$$\frac{\text{Cross-sectional area of fiber}}{\text{Cross-sectional area of tube}} \propto \frac{\dot{Q}_{Alg}}{\dot{Q}_{Total}} \propto \left(\frac{d_{fiber}}{D}\right)^2 \quad (1)$$

As we can write

$$\frac{\dot{Q}_{Alg}}{\dot{Q}_{Total}} = (1 + R^{-1})^{-1} \quad (2)$$

the fiber diameter can be predicted by using eqs. (1) and (2) as:

$$\left(\frac{d_{fiber}}{D}\right) = A(1 + R^{-1})^{-1/2} \quad (3)$$

In eq. (3),  $A$  is a fit parameter. We plot eq. (3) in Figure 3 and find that for  $A = 0.7$ , there is excellent agreement with the experimental data. Interestingly, eq. (3) predicts that when  $R \rightarrow 0$ ,  $d_{fiber} \rightarrow 0$  and when  $R \rightarrow \infty$ ,  $d_{fiber} \rightarrow A$ . These limits appear to be consistent with the experimental data.

Next, we evaluated the fiber production rate where we plot in Figure 4, the mean velocity of fiber normalized with the mean velocity corresponding to the total flow rate. It is evident from Figure 4 that the fiber production velocity is dependent on the flow rate ratio for both concentrations of CaCl<sub>2</sub>, with the higher concentration showing higher fiber velocity. In addition, we observe a maximum in the fiber velocity when  $R = 1$  for both

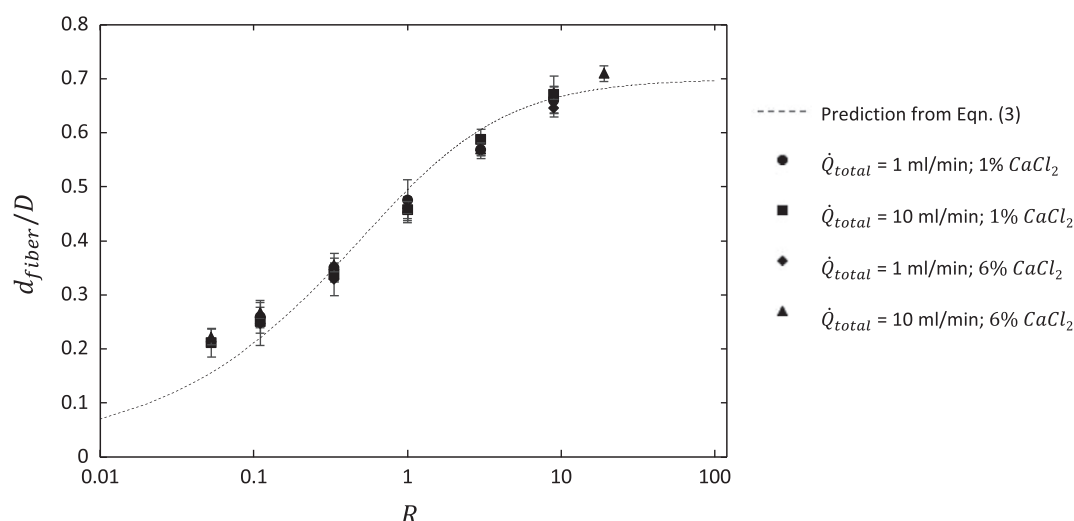


**Figure 3.** Dependence of the fiber diameter on flow rate ratio. The symbols are experimental data and the dashed line is the prediction from eq. (3). For these conditions, the exit channel length  $L = 20$  cm.

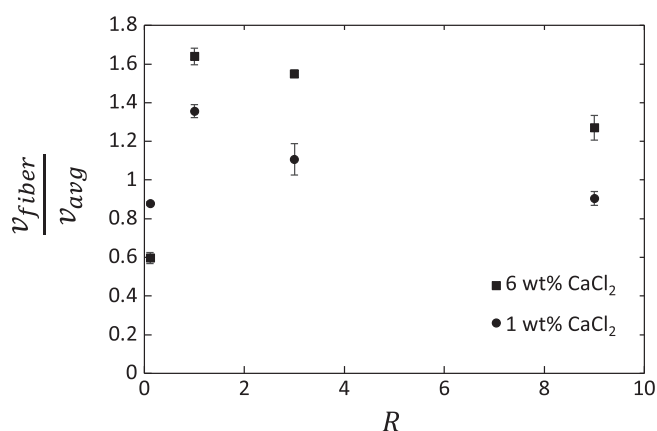


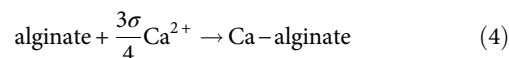
**Figure 4.** Normalized fiber velocity versus flow rate ratio at  $\dot{Q}_{\text{total}} = 1$  mL  $\text{min}^{-1}$  and  $C_{\text{CaCl}_2} = 1$  wt % (squares) and 6 wt % (circles). Here,  $L = 20$  cm.

cases. This observation can be explained by considering the location of the diffusive interface between the alginate and calcium chloride streams. At  $R = 1$ , we expect the interface to be at the center of tube [cf. Figure 1(c)] where the fluid velocity is maximum and may coincide with the crosslinked fiber front. However, at other flow rate ratios, the diffusive interface will be closer to the walls of the exit channel walls and therefore the crosslinked fiber front is expected to have a lower average velocity than that observed for  $R = 1$ . The higher fiber production rate corresponding to  $R = 1$  and 6 wt % calcium chloride was found to be  $9.8 \pm 0.2$  m  $\text{min}^{-1}$ .

#### Effect of Crosslinking Time on Fiber Quality

We have shown in Figure 2 that for the conditions where  $\dot{Q}_{\text{total}} > 10$  mL  $\text{min}^{-1}$ , nonuniform fibers are produced. The kinks in the fiber make them easily breakable [Figure 5(a)] and can occur if: (1) there is not enough calcium to crosslink the alginate, or (2) if calcium does not have enough time to crosslink the alginate. The amount of calcium ions required to crosslink the alginate is determined by the guluronic acid content in alginate.<sup>33</sup> If

the guluronic acid content is known, stoichiometry of alginate crosslinking reaction is given by the equation below<sup>34</sup>:



where  $\sigma$  corresponds to the guluronic acid content in the alginate.<sup>33</sup>

Alginate used in our studies has a ratio of mannuronic acid content to guluronic acid content of 1.56. Using the aforementioned equation, we find that sufficient calcium ions are present to completely crosslink all available alginate for all conditions under which fibers are produced at  $\dot{Q}_{\text{total}} > 10$  mL  $\text{min}^{-1}$  in Figure 2. We therefore hypothesize that the nonuniform fiber regime observed in Figure 2 are caused by insufficient time available for crosslinking.

To test this hypothesis, we chose the conditions where there is enough calcium to crosslink the alginate ( $R = 1$ ) and explore the effect of residence time in the exit channel (crosslinking time) on the occurrence of fiber nonuniformities. We achieve this by: (1) changing the exit channel length ( $L$ ) for a given  $\dot{Q}_{\text{total}}$ ; and (2) changing  $\dot{Q}_{\text{total}}$  for a fixed exit channel length ( $L$ ). Results of these studies are shown in Figure 5(b,c). We observed that for both 1 and 6 wt %  $\text{CaCl}_2$  reducing  $L$  at a given  $\dot{Q}_{\text{total}}$  produces nonuniform fibers. The same trend is observed when increasing  $\dot{Q}_{\text{total}}$  for a fixed  $L$ . Increasing the calcium chloride concentration increases the calcium ion diffusive flux and allows uniform fibers to be produced at shorter exit channel lengths. Thus, our observations in Figure 5 support our hypothesis that non-uniform fibers are produced due to insufficient time available for crosslinking and that this time can be manipulated by altering the exit channel length or residence times.

Our results thus far show that inadequate crosslinking time can lead to nonuniform fibers. Due to insufficient crosslinking time, fiber gelation does not reach completion. Therefore, the mechanical strength of the fiber is weak and prone to breakage. To identify the minimum mechanical strength necessary to obtain

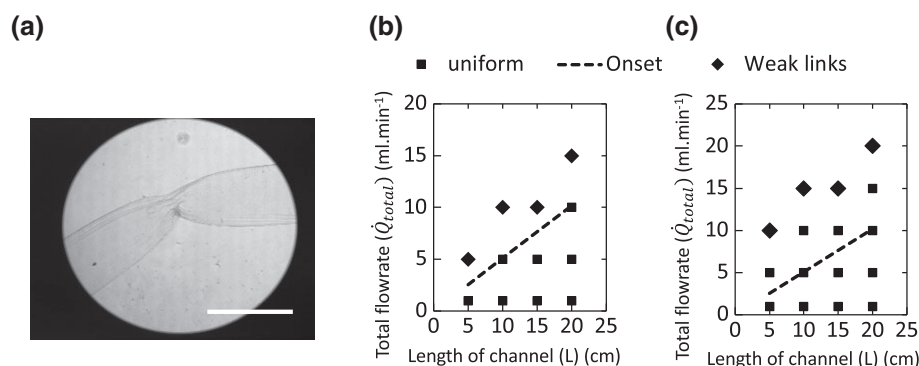


**Figure 5.** (a) Alginate fiber with weak links produced at  $\dot{Q}_{total} = 15 \text{ mL min}^{-1}$ ,  $L = 10 \text{ cm}$  and  $R = 1$  with 1 wt % calcium chloride. Transition of uniform fibers into fibers with weak links for (b) 1 wt % calcium chloride and (c) 6 wt % calcium chloride. Black filled squares (■) represent uniform fibers, black diamonds (◆) represent fibers with weak links, and black dashed line (---) represents the transition from uniform fibers to fibers with weak links.

uniform fibers, we use an empirical equation (eq. (5)) that correlates the storage modulus of alginate gels with crosslinking time.<sup>35–37</sup>

$$\frac{G'}{G'_{\infty}} = (1 - e^{-kt})^n \quad (5)$$

In the above equation,  $t$  is the amount of time alginate is exposed to calcium ions,  $G'$  is the storage modulus of alginate gel at  $t$ ,  $G'_{\infty}$  is the storage modulus of the same gel as  $t \rightarrow \infty$ ,  $k$  is the gelation rate constant, and  $n$  is the heterogeneous structural resistance constant. The  $k$  and  $n$  values for 1 wt % calcium chloride are reported to be  $0.015 \text{ s}^{-1}$  and 0.6, respectively.<sup>36</sup>

For our system,  $t = t_{res} = \frac{\pi d^2 L}{4 \dot{Q}_{total}}$ , which is the residence time of alginate in the exit channel. Using the reported values of  $k$  and  $n$ , and calculated values of  $t_{res}$  we find that the transition between uniform and nonuniform fiber regimes can be predicted as approximately  $\frac{G'}{G'_{\infty}} = 0.13$  for 1 wt %  $\text{CaCl}_2$  and for 6 wt %  $\text{CaCl}_2$ . This analysis supports our hypothesis that a minimum gel strength that is dependent on crosslinking time is necessary to create uniform fibers.

## CONCLUSIONS

We have demonstrated that continuous, clog-free, uniform alginate fiber production at a rate of  $\sim 10 \text{ m min}^{-1}$  is possible by using just syringe pumps, connecting tubes and a T-junction. Fibers with controlled diameters in the range of 300–1000  $\mu\text{m}$  can be produced reproducibly by adjusting the alginate-to-calcium chloride flow rate ratio ( $R$ ) between the values of 0.1 and 10. Fiber production rate also depends on flow rate ratio and is maximum when the flow rate ratio is unity. Uniform fibers are produced only if the alginate fibers develop adequate gel strength which is directly dependent on crosslinking time. Our simple and high throughput method for alginate fiber production may find potential applications in tissue engineering and wound management. Characterization of fiber morphology and mechanical properties is outside the scope of this work and should be the focus of future studies.

## REFERENCES

- Kamiya, R.; Cheeseman, B. A.; Popper, P.; Chou, T.-W. *Compo. Sci. Technol.* **2000**, 60(1), 33.
- Wang, X.; Han, C.; Hu, X.; Sun, H.; You, C.; Gao, C.; Haiyang, Y. *J. Mech. Behav. Biomed. Mater.* **2011**, 4(7), 922.
- Nichol, J. W.; Khademhosseini, A. *Soft Matter.* **2009**, 5(7), 1312.
- Kang, E.; Choi, Y. Y.; Chae, S. K.; Moon, J. H.; Chang, J. Y.; Lee, S. H. *Adv. Mater.* **2012**, 24(31), 4271.
- Qin, Y.; Agboh, C.; Wang, X. D.; Gilding, K. *Text. Magazine.* **1996**, 25, 22.
- Qin, Y. *Text. Res. J.* **2005**, 75(2), 165.
- Qin, Y. *Polym. Int.* **2008**, 57(2), 171.
- Zussman, E. *Polym. Adv. Technol.* **2011**, 22(3), 366.
- Tamayol, A.; Akbari, M.; Annabi, N.; Paul, A.; Khademhosseini, A.; Juncker, D. *Biotechnol. Adv.* **2013**, 31(5), 669.
- Reneker, D.; Yarin, A.; Zussman, E.; Xu, H. *Adv. Appl. Mech.* **2007**, 41, 43.
- Bhattacharai, N.; Zhang, M. *Nanotechnology.* **2007**, 18(45), 455601.
- Deng, M.; James, R.; Laurencin, C. T.; Kumbar, S. G. *IEEE Trans. Nanobioscience.* **2012**, 11(1), 3.
- Puppi, D.; Dinucci, D.; Bartoli, C.; Mota, C.; Migone, C.; Dini, F.; Barsotti, G.; Carlucci, F.; Chiellini, F. *J. Bioact. Compat. Polym.* **2011**, 26(5), 478.
- Lee, G.-S.; Park, J.-H.; Shin, U. S.; Kim, H.-W. *Acta Biomater.* **2011**, 7(8), 3178.
- Xu, G. K.; Liu, L.; Yao, J. M. *Fabrication and Characterization of Alginate Fibers by Wet-Spinning*. Vol. 796; *Adv. Mat. Res.*, **2013**. p. 87.
- Mazzitelli, S.; Capretto, L.; Carugo, D.; Zhang, X.; Piva, R.; Nastruzzi, C. *Lab Chip.* **2011**, 11(10), 1776.
- Su, J.; Zheng, Y.; Wu, H. *Lab Chip.* **2009**, 9(7), 996.
- Yamada, M.; Sugaya, S.; Naganuma, Y.; Seki, M. *Soft Matter.* **2012**, 8(11), 3122.



19. Jeong, W.; Kim, J.; Kim, S.; Lee, S.; Mensing, G.; Beebe, D. J. *Lab Chip*. **2004**, 4(6), 576.
20. Onoe, H.; Okitsu, T.; Itou, A.; Kato-Negishi, M.; Gojo, R.; Kiriya, D.; Sato, K.; Miura, S.; Iwanaga, S.; Kuribayashi-Shigetomi, K. *Nat. Mater.* **2013**, 12(6), 584.
21. Bonhomme, O.; Leng, J.; Colin, A. *Soft Matter*. **2012**, 8(41), 10641.
22. Shin, S.-J.; Park, J.-Y.; Lee, J.-Y.; Park, H.; Park, Y.-D.; Lee, K.-B.; Whang, C.-M.; Lee, S.-H. *Langmuir*. **2007**, 23(17), 9104.
23. Jeong, W. J.; Kim, J. Y.; Choo, J.; Lee, E. K.; Han, C. S.; Beebe, D. J.; Seong, G. H.; Lee, S. H. *Langmuir*. **2005**, 21(9), 3738.
24. Ghorbanian, S.; Qasaimeh, M. A.; Akbari, M.; Tamayol, A.; Juncker, D. *Biomed. Microdevices*. **2014**, 16(3), 387.
25. Wan, A. C.; Liao, I.-C.; Yim, E. K.; Leong, K. W. *Macromolecules*. **2004**, 37(18), 7019.
26. Wan, A. C.; Leong, M. F.; Toh, J. K.; Zheng, Y.; Ying, J. Y. *Adv. Healthc. Mater.* **2012**, 1(1), 101.
27. Yim, E. K. F.; Wan, A. C. A.; Le Visage, C.; Liao, I. C.; Leong, K. W. *Biomaterials*. **2006**, 27(36), 6111.
28. Wan, A. C.; Tai, B. C.; Leck, K. J.; Ying, J. Y. *Adv. Mater.* **2006**, 18(5), 641.
29. Takei, T.; Sakai, S.; Ijima, H.; Kawakami, K. *Biotechnol. J.* **2006**, 1(9), 1014.
30. Tamayol, A.; Akbari, M.; Annabi, N.; Paul, A.; Khademhosseini, A.; Junker, D. *Biotechnol. Adv.* **2013**, 31, 669.
31. Bui, A. V.; Nguyen, M. J. *Food Eng.* **2004**, 62(4), 345.
32. Robinson, R.; Chia, C. J. *Am. Chem. Soc.* **1952**, 74(11), 2776.
33. Morris, E. R.; Rees, D. A.; Thom, D.; Boyd, J. *Carbohydr. Res.* **1978**, 66(1), 145.
34. Braschler, T.; Valero, A.; Colella, L.; Pataky, K.; Brugger, J. r.; Renaud, P. *Anal. Chem.* **2011**, 83(6), 2234.
35. Lee, P.; Rogers, M. *Int. J. Gastron. Food Sci.* **2012**, 1(2), 96.
36. Chrastil, J. *J. Agric. Food Chem.* **1991**, 39(5), 874.
37. Chrastil, J. *J. Agric. Food Chem.* **1990**, 38(9), 1804.